HHS Public Access

Author manuscript

*Am J Rhinol Allergy*. Author manuscript; available in PMC 2018 April 17.

Published in final edited form as:

*Am J Rhinol Allergy*. 2010 ; 24(2): 110–120. doi:10.2500/ajra.2010.24.3435.

# Neuropathology of the Olfactory Mucosa in Chronic Rhinosinusitis

**Karen K. Yee, Ph.D.**[1,*], **Edmund A. Pribitkin, M.D.**[1,2], **Beverly J Cowart, Ph.D.**[1], **Aldona A. Vainius, B.S.**[1], **Christopher T. Klock, B.S.**[1], **David Rosen, M.D.**[2], **Pu Feng, Ph.D.**[1], **Judith McLean, Ph.D.**[1], **Chang-Gyu Hahn, M.D., Ph.D.**[3], and **Nancy E. Rawson, Ph.D.**[1,4]

[1]Monell Chemical Senses Center, 3500 Market Street, Philadelphia, PA 19104-3308

[2]Otolaryngology-Head & Neck Surgery, Thomas Jefferson University, Philadelphia, PA

[3]Department of Psychiatry, University of Pennsylvania, Philadelphia, PA

## Abstract

**Background/Objective—**Chronic rhinosinusitis (CRS) is a complex heterogeneous inflammatory disease that affects the nasal cavity, yet the pathological examination of the olfactory mucosa (OM) in this disease has been limited.

**Methods—**Nasal biopsies were obtained from 20 control subjects and 50 CRS patients in conjunction with clinical assessments. Histopathology of these nasal biopsies was performed and immunohistochemistry was used to characterize non-neuronal, neuronal and inflammatory cells in the OM. These OM characteristics were then evaluated to determine the degree to which pathological features may be related to smell loss in CRS.

**Results—**Histopathological examination of control and CRS OM revealed changes in the normal pseudostratified olfactory epithelium (OE): intermixing of goblet cells, metaplasia to squamous-like cells, and erosion of the OE. Lower percentages of normal epithelium and olfactory sensory neurons were found in CRS OE compared with controls. Relative to other CRS patients, those with anosmia had the greatest amount of OE erosion, the highest density of eosinophils infiltrating the OE and exhibited the most extensive abnormalities on CT and endoscopic examination, including being significantly more likely to exhibit nasal polyposis.

**Conclusion—**Our results suggest that OM pathology observed in nasal biopsies can assist in understanding the degree of epithelial change and sensorineural damage in CRS and the potential for olfactory loss.

### Keywords

Olfaction; human; nasal; clinical; olfactory epithelium; immunohistochemistry; histopathology; biopsy; repair; hyposmia

[*]Corresponding author, Karen K. Yee, Monell Chemical Senses Center, 3500 Market St., Philadelphia PA 19104-3308, Phone: 267-519-4823, Fax: 215-898-2084, karenyee@monell.org.

[4]Current address: WellGen, Inc., Commercialization Center for Innovative Technologies, 675 US Highway One, North Brunswick, NJ 08902

We have no conflict of interest nor have financial disclosure to report.

Human protocols used in this study were approved by the Institutional Review Board of Thomas Jefferson University.

## INTRODUCTION

Chronic rhinosinusitis (CRS) is a primary cause of olfactory loss among patients presenting to chemosensory clinics[1], and is the most common chronic medical condition in the United States, affecting an estimated 33 million people/year.[2] Adult CRS is defined by the Sinus and Allergy Health Partnership Task Force as prolonged rhinosinusitis symptoms (e.g., nasal congestion, facial pain/pressure, and nasal discharge/purulence) persisting for greater than 12 weeks.[3] It is currently debated whether CRS should be subdivided into CRS with and without allergies, nasal polyps, or eosinophilia.[4] It has been reported that 25–30% of CRS patients experience moderate to severe olfactory impairment.[5] Unfortunately, olfactory loss and likelihood of recovery often fails to correlate with clinical observations of nasal congestion or symptom severity[6], and there are presently no reliable criteria for predicting either the likelihood of olfactory loss over time, or its recovery upon treatment.

The cause of olfactory loss in CRS has been attributed to conductive (airflow impairment) and sensorineural (damage to the olfactory epithelium) factors, and it is likely that both factors contribute to varying degrees.[7] The likelihood of recovery upon resolution of airflow restriction (via, for instance, surgery or steroid application) would seem to be dependent upon an intact olfactory mucosa (OM), whereas extensive damage to sensory structures would produce a more severe or intractable olfactory loss. An understanding of basic mammalian OM cellular composition and physiology is required to assess the causes of olfactory dysfunction. The olfactory epithelium (OE) is composed of an apical layer of olfactory sustentacular cells and several layers of mature and immature olfactory sensory neurons (OSNs) that are true bipolar neurons consisting of both a dendrite that extends beyond the apical surface, where its cilia project into the mucus layer, and a basally projecting axon process.[8] Odorants bind to over 400 olfactory receptors expressed in the cilia of human OSNs[9] and activate second messenger G-protein mediated signaling[10] that is relayed to the olfactory bulbs, the primary olfactory cortex and higher cortical regions.[11] Above the basement membrane (BM) is a layer of proliferative basal cells that support continuous neurogenesis throughout the life of the animal.[12] The underlying lamina propria is composed of collagen, blood vessels, serous and acinar glands, axonal bundles, trigeminal fibers, native immune cells, and cartilage of the turbinate. The respiratory epithelium (RE) is characterized by a single apical layer of respiratory cells with microvillar processes, the presence of goblet cells, and 1–2 layers of basal cells.[8]

There are, however, differences in morphology and the localization of sensory OM between non-human mammals and humans. In rodents, the sensory OM lines specific regions of the endoturbinates, ectoturbinates, and septum,[13] and as the animal matures, the OE increases in thickness and cells come to be arranged in a laminar organization. The human nasal cavity is less convoluted and composed of only three turbinates (i.e., superior, middle and inferior) and sensory OM resides predominantly on the superior turbinate[14, 15], although other studies indicate that sensory OM may also extend anteriorly to the upper aspects of the middle turbinate and the apposed septum. [16–18] Unlike the rodent, human OE decreases in thickness with age, lacks the distinctive laminar organization and displays varying degrees of

neuroepithelial degeneration depending on injury, infection, chemical exposures, nasal surgery, or age-related phenomena.[19]

Numerous studies have examined histopathological and inflammatory parameters of RE or sinonasal tissue from CRS patients grouped in specific subtypes (e.g., with or without nasal polyps or allergies).[20–25] Extensive chronic inflammation is evident in the sinonasal tissue, with high eosinophilic infiltration associated with nasal polyps. Very few studies have examined the morphology and neuronal profile of the sensory OM in CRS. In a qualitative study, all CRS patients with impaired olfaction exhibited moderate or severe inflammatory changes in the OM, whereas only 40% of patients with normal olfaction exhibited moderate pathology and none exhibited severe pathology.[26] The study also found that degenerated OE was particularly evident in regions of inflammation within the lamina propria, indicating that sensory damage was a contributing factor to secondary smell loss in CRS. An immunohistochemical study examining specific markers for OSNs demonstrated changes to sensory OM in various nasal disorders.[27] Regions of OE intermingled with RE, degeneration of OE with few, scattered mature OSNs, a predominance of immature OSNs, the presence of neuromas, and empty nerve fascicles were evident in both normosmic and hyposmic patients. The results from these studies suggest sensorineural damage may contribute to olfactory loss.

The present study was undertaken to characterize the general histopathology and inflammatory state of the OM in controls as compared to CRS patients and to assess whether the observed histopathologies of OM, based on blinded clinical classification, may offer insight into the nature of OM damage occurring in patients with varying degrees of disease severity and olfactory function, providing a foundation for the prognosis for olfactory loss or recovery. A particular limitation is the degree to which these data, derived from biopsies from a limited region, may represent the entire nasal cavity or sensory epithelial sheet. Nevertheless, our results provide a snapshot of human sensory OM and reveal the dynamic and heterogeneous morphological changes that can occur as it undergoes inflammatory and regenerative processes. Preliminary findings from this study have been presented in abstract form[28–31] and in a symposium.[32]

## METHODS AND MATERIALS

### Subjects

The patient population was drawn from the Otolaryngology-Head & Neck Surgery Department at Thomas Jefferson University, which evaluates over 700 new patients for sinus-related disease in a given year. We recruited adult subjects according to the criteria developed by the Sinus and Allergy Health Partnership Task Force for adult CRS.[3] We report data from 50 CRS patients (12M and 38F) ranging in age from 18–58 years old (mean ± sem, 41.0 ± 1.7) who volunteered between July 2005 – March 2008, excluding four patients >60 years old. CRS patients were asked to refrain from using nasal/sinus medications, beta blockers and tricyclic antidepressants for 4 days prior to testing. Patients underwent nasal endoscopy and computed tomography, with scores based on the University of Miami CRS staging system[33] tabulated by EAP and DR. In addition, patients were given a 24-allergen prick test (Multi-Test®II, Lincoln Disagnostics INC, Decatur, IL), and

extensive information was collected on general medical history, subjective symptoms, psychological profile, quality of life and chemical exposure history for each patient. Included in our patient group were three patients with nasal polyps based on their nasal endoscopic examination, 13 patients with at least one positive response on the allergy test, and eight current smokers.

We also recruited controls in good health as determined by responses to a questionnaire, who had no self-reported history of sinus disease or inhalant allergies, and who performed within normal limits on an olfactory detection threshold task. Controls did not undergo allergy prick testing. Excluded from this study were one control who exhibited diminished olfactory sensitivity on the threshold task and two controls with visibly inflamed nasal tissue as determined during endoscopic examination. We report on 20 controls (5M and 15F) ranging in age from 19 – 56 years (mean, 33.6 ± 2.3), including two who were current smokers. There was a significant difference between the ages of the CRS patients and control subjects ($t=2.37$, $p<0.05$).

## Olfactory Threshold Task

Olfactory thresholds were determined for phenylethyl alcohol (PEA), which has been reported to elicit little or no trigeminal response at any concentration.[34–36] The PEA threshold series consisted of 20 concentrations beginning with a neat solution (step 0) and extending in half-log dilution steps to a concentration of −9.5 log vol/vol (step 19). PEA was diluted in glycerol, which also served as a blank. Thresholds were determined using a two-alternative, forced-choice, staircase procedure.[37] Details of our current threshold criteria can be found in Pribitkin et al.[38] A PEA dilution step ≥8 (≤−4.0 log vol/vol) was considered to be within normal olfactory threshold limits.[39, 40] Thresholds were assessed separately in each nostril, and we report the poorest threshold value obtained by each participant.

## Nasal Biopsies

Following informed consent, 1–2$mm^3$ biopsies were taken under local anesthesia by EAP or DR in the physician's examination room, following protocols approved by the Institutional Review Board of Thomas Jefferson University. One biopsy was collected from the upper aspect of the middle turbinate and one from the apposed septum on the nasal side with the worst PEA score as described above. The precise area where the biopsies were taken was dependent on accessibility of the nasal cavity in each individual. This biopsy technique has been performed on over 500 subjects in our clinic without serious adverse events.

For the initial 30 CRS patients and three controls, both biopsies were randomly processed for frozen and paraffin sections to assay the optimal conditions for various antibodies. Gross histopathological evaluation found that 54.5% of septal biopsies yielded >50% RE, comprised primarily of Alcian Blue stained goblet cells, while only 33.3% of turbinate biopsies exhibited this appearance. Given these results, the middle turbinate biopsies for the remaining subjects were processed for frozen sections, and septal biopsies were either stored or used for other experiments. To avoid inconsistencies due to different processing methods, we analyzed only the biopsies that were processed for frozen sections: 59 middle turbinate biopsies (40 patients and 19 controls) and 11 septal biopsies (10 patients and one control).

## Tissue Preparation and Histological Staining

Biopsies were immediately placed in 4% paraformaldehyde for 1–2 hr, processed through a series of 10–30% sucrose solutions for crytoprotection, and then rapidly embedded in M1 matrix medium (Shandon) using a dry ice acetone bath. Care was taken during processing to insure minimal tissue damage due to handling. The biopsies were positioned and cut at a thickness of 10μm through the entire tissue to yield sections with similar orientations, mounted on StarFrost slides (Mercedes Medical, Sarasota FL) and stored at −20°C until used. From each biopsy, three slides equally spaced apart (approximately 300 – 450μm depending on the number of slides generated) were stained in succession with Alcian Blue (pH 3.0, Sigma, St. Louis, MO) to identify acidic mucus in the OE and glands, Harris modified hematoxylin (Fisher Scientific, Pittsburg PA), and eosin (Sigma) to identify cell nuclei and tissue structures in the olfactory mucosa.

## Immunohistochemistry and Imaging

Neuronal and non-neuronal primary antibodies used in this study are listed in Table 1. For characterizing neuronal cells, we used olfactory marker protein (OMP) antibody, which is a polyclonal goat antiserum generated against OMP whole protein purified from rat (generous gift of Dr. Frank Margolis and purchased from Wako, Richmond, VA) [41], a rabbit polyclonal Protein Gene Product 9.5 (PGP9.5 = ubiquitin carboxy-terminal hydrolase L1, UCHL1, Chemicon, Temecula, CA)[42] as a supporting neuronal marker for olfactory neurons, axons and trigeminal fibers[43], a mouse monoclonal anti-growth associated protein 43 antibody (GAP43, Sigma) that labels immature OSNs,[44] and a mouse monoclonal anti-neuronal class III β-tubulin (NST Covance, Berkeley, CA) antibody raised against microtubules derived from rat brain that recognizes the epitope CEAQGPK in the carboxyl-terminus of class III β-tubulin.[45] It has been characterized in humans[46] to label OSNs, however in our hands, the antibody only identified olfactory axonal bundles and trigeminal nerves in frozen sections as processed in this study. Basal cells were identified with mouse monoclonal anti-p75 nerve growth factor receptor (p75NGFR, Chemicon)[47] A rabbit polyclonal anti-Ki67 (Labvision, Frement, CA) was used to detect proliferating basal cells. Olfactory sustentacular cells and mucus glands were identified with two biomarkers: a monoclonal mouse cytokeratin 18 (Chemicon)[48, 49] and a polyclonal rabbit cytochrome 2A5 (cyp2A5) that was developed by Dr. XinXin Ding specifically to recognize both mouse cyp2A and cyp2G, and human cyp2A (in humans cyp2G is a pseudogene).[50]

Standard immunohistochemical techniques were used. Briefly, oven dried frozen sections were rehydrated with 0.1M phosphate buffer solution (PBS) at pH 7.0. Endogenous peroxidase was blocked by 3% $H_2O_2$, and nonspecific binding was blocked with Superblock (Pierce). Sections were incubated with primary antibody overnight at 4°C in a humidified chamber followed by secondary biotinylated antibody and avidin-biotinylated horseradish peroxidase complex (ABC Elite Kit, Vector Laboratories, Burlingame, CA) and reacted with chromogen diaminobenzidine (DAB, Sigma Chemicals) for visualization. Antigen retrieval with citrate buffer pH 6.0 at 95°C was performed for CK18, Ki67, and cyp2A5 antibodies. All double immunofluorescence labeling studies were done in series with appropriate second primary antibodies (Alexa488 donkey anti-goat, Alexa555 donkey anti-mouse, and

Alexa647 donkey anti-rabbit; Molecular Probes, Eugene, OR), and DAPI (dilution 1:1000, Molecular Probes) was used to label cell nuclei.

Specific biomarkers used to identify eosinophils (major basic protein, MBP), macrophages (CD64) and neutrophils (elastase) are also listed in Table 1 and were all purchased from BD Biosciences (San Jose, CA). Similar immunohistochemical techniques as described above were used with host-specific secondary kits (BD Biosciences), and sections were counterstained with hematoxylin to aid in cellular visualization. Negative controls included the omission of primary antibody and incubation with appropriate IgG. Since subjects were recruited over a period of time, biopsies were stained and processed for all antibodies simultaneously to prevent variability due to multiple staining batches.

Brightfield images were captured using a SPOT digital camera (Diagnostic Instruments, Inc) attached to a Nikon SA Microphot microscope and minimally processed using Image-Pro Plus image analysis software (Media Cybernetics Inc., Silver Spring, MD). Fluorescent images were captured with the Leica TCS SP2 Spectral Confocal Microscope (Leica Microsystems Inc., Mannheim, Germany) using UV, Ar, GeNe and HeNe lasers and appropriate excitation spectrums. Leica Scanware software was used to acquire z-series stacks captured at a 0.4μm step size. Digital images were cropped, arranged and minimally adjusted for contrast and brightness for background standardization using Photoshop CS (Adobe Systems, Inc., San Jose, California).

## Epithelial Assessments

KKY and NER evaluated histological stained sections to establish standards for assessment of sensory OM histomorphological characteristics with respect to the cellular organization and identification of the cell types (neuronal and non-neuronal). Three histologically stained sections from each biopsy was then examined by KKY and JM independently while blinded to the clinical details of the subject and classified according to the epithelial morphology (i.e., normal pseudostratified, intermixing of goblet cells, squamous metaplasia, and erosion) that predominated in the biopsy. The two reviewers agreed on 81.8% of the biopsies; the 10 biopsies that were scored differently were re-examined to reach an agreed-upon predominant morphology. OE with damage that in KKY's judgment was due to handling during the biopsy procedure, freezing or sectioning were not included in the analysis.

## Quantitative Analyses

The distribution frequency of the different epithelial morphologies in each biopsy was quantitatively analyzed using ImagePro Plus image analysis software; the relative percentages of the different morphologies were determined (the length of an epithelial morphology type/the total OE length of the biopsy) for three histologically stained sections/biopsy and averaged for specific groups.

Due to the heterogeneity of the OE morphology, we relied on biomarkers of OSNs (OMP and PGP9.5) and olfactory sustentacular cells (CK18) to assist in the identification of sensory epithelium. Immunohistochemical experiments using both DAB and double immunofluorescence labeling were performed on several adjacent sections for each biopsy. Only nasal biopsies with regions of sensory OE with identifiable normal or abnormal ONSs

were analyzed for this study. Cells exhibiting OMP-ir and PGP9.5-ir that were located near the basement membrane or lacked the classical shape of cell body with dendritic and axonal processes were defined as morphologically abnormal OSNs. RE can often intermix in the regions of human sensory OE and may be difficult to distinguish. Our criteria for RE were: the lack of OMP, PGP9.5, or CK18 immunoreactivity (ir) with or without the presence of goblet cells. Regions of epithelium that met these criteria were not analyzed in this study.

For quantitative morphometric measurements, three regions of the OE and underlying lamina propria were imaged at 20X for each histologically stained section and demarcated using ImagePro Plus software. OE and BM thicknesses were manually measured and average thicknesses calculated. Also within each region of OM, a 200μm$^2$ area of interest below the BM was demarcated; the total number of visible mucus glands and blood vessels were counted and the average density/200μm$^2$ was calculated for both. Overall, 6–9 regions of OM were measured for each subject, depending on the size of the biopsy. The number of infiltrating eosinophils, macrophages, and neutrophils were manually counted over the entire length of OE (cells/mm) under the microscope with a 20X – 40X objective to determine the density of the immune cell population.

### Statistical Analysis

The data were assessed initially using summary statistics such as means, standard errors, and frequencies; in addition, correlations and cross-tabulations among key factors were conducted. Morphological and clinical characteristics were compared across control and CRS groups (defined by predominant OE morphological type and olfactory performance) using Fisher's exact test for categorical variables and t-tests or one-way analysis of variance (ANOVA) for continuous data, with the latter followed by post-hoc pairwise comparisons using Fisher's LSD. Percent values characterizing OE morphology were arcsin transformed prior to parametric analyses, as recommended by Winer[51]; however, untransformed percents are presented in the tables for ease of interpretation (the transformation did not substantially alter the results of any analysis). T-test, ANOVA, 2×2 Fisher's exact, and Fisher's LSD tests were conducted using Statistica (v8.0 StatSoft, Inc., Tulsa, OK). Fisher's exact values for larger contingency tables were calculated using online statistical programs [Simple Interactive Statistical Analysis (SISA): Uitenbroek DG, 2000, www.quantitativeskills.com/sisa/statistics/fiveby2.htm, or VassarStats: Lowry R, 1998, faculty.vassar.edu/lowry/VassarStats.html]. A p value ≤0.05 was considered to be statistically significant for all analyses.

## RESULTS

### Epithelial Morphology of Nasal Biopsies

Epithelial examination of histologically stained sections revealed a heterogeneous OE comprised of several different morphologies in both control and CRS biopsies: normal pseudostratified, OE intermixed with goblet cells, squamous metaplasia, and erosion (Figure 1). Normal pseudostratified OE was composed of multiple layers of cells with a distinct basal cell layer and a layer of apical sustentacular cells with microvilli (further identified by immunohistochemistry) in both control (Fig 1A) and CRS biopsies (Fig 1B). Regions

comprising Alcian Blue-stained goblet cells interspersed with pseudostratified OE were also observed occasionally in control (Fig 1C) and in CRS biopsies (Fig 1D).

A shift from pseudostratified epithelial layers into stratified squamous-like cells, exhibiting the distinctive cuboidal shape, was observed to various degrees from mild (Fig 1E) to moderate squamous metaplasia with increasing epithelial thickness (Fig 1F) in control biopsies. In CRS biopsies, moderate squamous metaplasia was often accompanied by invagination of the lamina propria into the OE (Fig 1G). More severe squamous metaplasia, with multiple layers of flattened cells, was observed only in CRS biopsies (Fig 1H).

The OE was considered eroded based on the loss of cellular layers and/or a loose epithelial matrix (Fig 1I). The degree of erosion was more severe in CRS biopsies than in those of controls, sometimes leaving only the remnants of the basal cell layer or an exposed BM (Fig 1J). Regions with a high density of Alcian Blue-stained goblet cells (Fig 1K) that lacked sustentacular or neuronal cells (not detected by immunohistochemistry) were identified as RE and were not analyzed.

## Identification of Olfactory Mucosa in Nasal Biopsies

Since the identification of the OE based on morphology was difficult, we relied on specific biomarkers to identify OSNs, which had specific cellular characteristics and varied in protein expression depending on the different types of epithelial morphology. Layers of bipolar OMP-ir OSNs were observed in normal OE of both control (Fig 2A) and CRS biopsies (Fig 2B). In OE intermixed with goblet cells in both sets of biopsies, OMP-ir cells were still present though with less distinguishable OMP labeled processes (Fig 2C–D). We also conducted double immunofluorescence labeling with PGP9.5 and found the expression of OMP and PGP9.5 proteins varied in mature OSNs. Fig 2E–F illustrates OMP-ir cells labeled with PGP9.5, especially in the neuronal processes. In another OE region of the same control biopsy, a few OMP-ir cells with PGP9.5 labeled processes were observed among PGP9.5-ir cells. More typical of our biopsies was the observance of mature OMP-ir OSNs in patches or scattered throughout the OE, which is similar to other descriptions of human OE in various disease states.[27, 52] In an OE region with scattered neurons, a few OMP-ir cells with no PGP9.5 labeling were observed, suggesting a cellular alteration in protein expression. Olfactory neurogenesis is still on-going in these biopsies, as we also observed both immature GAP43-ir and mature OMP-ir OSNs (Fig 2I – J).

Squamous transformation disrupted the organization and cellular morphology of OSNs. In mild squamous metaplasia, OMP-ir OSNs were observed in multiple layers of the OE (Fig 3A) and near the BM, just above a layer of NGFR-ir basal cells (Fig 3B). In CRS biopsies with moderate to severe squamous metaplasia, the morphological shape of mature OSNs becomes abnormal, with no discernible dendrites or axons, and they are scattered in the squamous OE (Fig 3C). These abnormally shaped OSNs were unlikely to be functional. In adjacent sections of the same biopsy, immature GAP43-ir cells were observed among a few OMP-ir cells (Fig 3E) and a few GAP43-ir cells were labeled weakly with PGP9.5 (Fig 3F), illustrating ongoing neuronal differentiation in moderate squamous OE. In a CRS biopsy with severe squamous metaplasia, scattered PGP9.5-ir cells were observed with a few labeled weakly with OMP (Fg 3F, arrow). The immunoreactive staining of flattened layers

of cells at the apical surface may be transformed neurons still expressing neuronal protein, remnants of neuronal debris, or nonspecific staining of the apical edge of the biopsy.

## Cellular Characteristics in Nasal Biopsies

In normal pseudostratified OE, CK18-ir sustentacular cells were located in the apical layer with visible processes extending towards the BM (Fig 4A) and CK18-ir was also localized in Bowman's glands and mucus glands (data not shown). CK18-ir sustentacular cells co-localized with cyp2A5, which was particularly abundant in the cilium as reported previously (Fig 4B)[50]. Figure 4C illustrates the presence of OMP-ir OSNs with CK18-ir sustentacular cells, which suggests that CK18-ir could be used to assist in identifying sensory OE in the nasal biopsies. Although no CK18 labeling was observed in squamous OE, it is unknown if olfactory sustentacular cells are still present after squamous transformation. In eroded OE, the presence of CK18-ir sustentacular cells was dependent upon the severity of erosion (data not shown).

Olfactory nerve bundles in the lamina propria and trigeminal nerve fibers innervating the OE were identified with NST (Fig 4D) and PGP9.5 antibodies (data not shown). Unlike what has been reported in tissue from the superior turbinate[26, 27], olfactory nerve bundles were small and scattered in our nasal biopsies, which probably relates to the scattered and patchy regions of OSNs. A few NST-ir cells were also observed in the OE; however, this particular NST antibody in our hands did not label OSNs in most of the frozen nasal sections, even though OMP-ir OSNs were present. Very few Ki67-ir cells were observed in normal OE and goblet cells/intermixed OE (data not shown). In squamous metaplasia, a higher frequency of Ki67-ir cells was found in several layers above the basal cell layer (Fig 4E), indicating cells in the active phases of the cell cycle. In eroded OE where some cell layers were still present, an increase in Ki67-ir cells was sometimes observed (data not shown).

## Quantitative Analyses of Nasal Biopsies

The quantitative results of OE morphology, measurements and immune cell profiles for control and CRS biopsies are shown in Table 2. The percentages of the four specific OE morphologies/total OE were averaged for each group. There was a significantly lower percentage of normal OE in CRS biopsies than in control biopsies ($t=-2.53$, $p=0.01$), whereas the percentages of goblet cells/intermixed OE ($t=0.72$, $p=0.47$) and squamous OE ($t=-0.44$, $p=0.66$) were similar in both groups. Although the percentage of eroded OE in CRS biopsies was slightly higher than in control biopsies, the difference was not significant ($t=1.08$, $p=0.28$). Consistent with a disruption of normal OE protection and repair processes in CRS, there was a tendency toward greater heterogeneity in control than in CRS biopsies, with 65% of control vs. 42% of CRS biopsies exhibiting at least three of the different epithelial morphologies (Fisher's exact, $p=0.07$).

Immunohistochemical analysis revealed that normal OMP-ir OSNs with identifiable processes tended to be more prevalent in control than in CRS biopsies (Fisher's exact, $p=0.08$). 20% of control biopsies and 34% of CRS biopsies had no visible OMP-ir OSNs (Fisher's exact, $p=0.12$); however, PGP9.5-ir OSNs were present in all of these biopsies, indicating the presence of OE. ANOVAs of OE thickness, BM thickness, density of blood

vessels, and density of mucus glands revealed no significant differences between controls and CRS patients in these OM characteristics. Analysis of the inflammatory response revealed that the number of eosinophils tended to be higher in CRS OE relative to control OE ($t=1.72$, $p=0.09$). Unexpectedly, there were significantly more macrophages ($t=-2.03$, $p=0.046$) and a somewhat higher number of neutrophils ($t=-1.66$, $p=0.10$) in the control OE.

## Quantitative Analyses of Nasal Biopsies Based on Predominant Epithelial Morphology

Control and CRS biopsies were grouped according to predominant epithelial morphology (i.e., the largest percentage of total OE in each biopsy) for further characterization (Table 3). Only two control biopsies had >50% normal OE; these were not included in analyses due to the small sample, but their data (CON-NORM) are also shown in Table 3. Where overall group analyses were significant, the results of post-hoc pairwise comparisons are indicated in Table 3. Differences among groups in the percentages of goblet intermixed, squamous and eroded OE are as would be expected given the criterion for group assignment. In addition, the percentages of normal OE differ significantly among the five groups ($F=3.26$, $p=0.017$). Specifically, whereas control goblet (CON-GB), control squamous (CON-SQ) and CRS-GB groups exhibited similar percentages of normal OE, these percentage levels are significantly lower in the CRS-SQ and CRS-erosion (CRS-ER) groups. Since normal OE corresponds to the presence of mature OSNs, there was also a significant difference among the groups in the numbers of biopsies exhibiting normal OMP-ir OSNs (Fisher's exact, $p<0.001$), with a similar pattern of pairwise differences evident in post-hoc comparisons.

OE thickness is significantly different among the groups ($F=4.89$, $p=0.002$), primarily reflecting the thinner OE observed in the CRS-ER group. Analyses of BM thickness ($F=0.28$, $p=0.87$) and mucus gland density ($F=2.38$, $p=0.06$) did not reveal any differences among groups. However, specific changes in blood vessel density ($F=3.40$, $p=0.013$) are evident across different epithelial morphologies. Specifically, the lamina propria was more vascularized in CON-SQ and CRS-SQ groups than in the others. It may be that much of the impact of CRS on the lamina propria occurs more than 200$\mu m^2$ below the BM, and additional qualitative analysis of the different types of remodeling that may occur in the lamina propria, such as fibrosis and atrophy, could reveal additional OM differences between CRS groups.

Quantitative analyses also revealed significant group differences in the densities of eosinophils ($F=4.33$, $p=0.004$), macrophages ($F=8.75$, $p<0.001$), and neutrophils ($F=5.87$, $p<0.001$). Eosinophil density was elevated in CRS-ER patients relative to all other groups. The CON-SQ group showed the highest levels of both macrophages and neutrophils, indicating local acute inflammation of the OE in healthy subjects that may not be obvious during endoscopic examination. Relatively high mean levels of the latter two immune cell types were also observed in the CRS-ER group, but the variance observed in this group was also unusually high. The CON-GB and CRS-GB groups exhibited similar, sparse immune cell profiles, suggesting that an ongoing, low-level presence of immune cells is an element of the normal protective mechanisms present in healthy noses.

## Clinical Assessments and Morphological Comparison Based on Worst Olfactory Performance in CRS Patients

To determine if morphological or other clinical findings were associated with smell loss in CRS, patients were grouped according to the worst of their unilateral PEA detection scores (i.e., anosmic, PEA = 0; hyposmic, PEA >0 and <8; and normosmic, PEA ≥8). The clinical data and assessments for the three CRS groups, and controls where applicable, are given in Table 4, as are the results of post-hoc pairwise comparisons between groups when overall analyses indicated there were significant group differences. There were no differences in age ($F=2.40$, $p=0.76$) or the proportions of current smokers (Fisher's exact, $p=0.54$) among the control and the three CRS groups. CRS normosmics had an average 'worst PEA' score similar to that of controls. The proportions of patients who tested positive in the allergy skin test were similar for all CRS groups (Fisher's exact, $p=0.09$). There were significant differences in disease duration ($F=4.09$, $p=0.02$) with, surprisingly, the CRS anosmics reporting the shortest symptom durations and CRS normosmics the longest. This difference was not due to age, as the CRS anosmics were slightly older than the CRS normosmics. There were no differences among the three CRS groups in the frequency of reports of symptoms of congestion (Fisher's exact, $p=0.67$), facial pain (Fisher's exact, $p=0.16$), headaches (Fisher's exact, $p=0.90$), post nasal drip (Fisher's exact, $p=0.78$), or runny nose (Fisher's exact, $p=0.83$).

We also analyzed physical variables assessed in the endoscopic and CT examinations that were likely to contribute to olfactory dysfunction. CRS groups differing in olfactory function also differed in the frequency with which polyps were diagnosed (Fisher's exact, $p<0.001$), total endoscopic scores ($F=18.98$, $p<0.001$), CT scores for the anterior ($F=18.76$, $p<0.001$) and posterior ethmoids ($F=26.11$, $p<0.001$), and total CT scores ($F=12.97$, $p<0.001$). CT scores of more peripheral sinuses less likely to impact olfaction (e.g., maxillary, sphenoid and frontal, data not shown) were also significantly different among the CRS groups. In all cases, overall differences were driven by elevated scores in the CRS anosmics relative to the CRS normosmics and hyposmics, whose scores were similar. Analysis of prior nasal surgeries found no significant differences in septum repair (Fisher's exact, $p=0.75$), polypectomy (Fisher's exact, $p=0.54$), rhinoplasty (Fisher's exact, $p=1.00$), or sinus surgery (Fisher's exact, $p=0.38$) among the CRS groups differing in olfactory sensitivity.

Analyses of the four OE morphologies revealed significant group differences in the percentages of normal OE ($F=2.91$, $p=0.04$) but not in the percentages of goblet/intermixed OE ($F=0.28$, $p=0.84$), squamous OE ($F=0.37$, $p=0.78$), or eroded OE ($F=1.15$, $p=0.34$). All CRS groups had apparently lower percentages of normal OE than the controls, but only that of the anosmics was significantly lower (Fisher LSD, $p=0.01$), suggesting the loss of normal OE may contribute a sensorineural factor to olfactory dysfunction in these patients. Immune cell analyses revealed significant group differences in the densities of eosinophils infiltrating the OE ($F=5.18$, $p=0.003$), but not in the densities of macrophages ($F=1.67$, $p=0.18$) or neutrophils ($F=1.00$, $p=0.40$), suggesting an adverse impact of eosinophilic infiltration on the integrity of the sensory epithelial tissue.

## DISCUSSION

We acknowledge the difficulty in correlating olfactory ability or dysfunction with nasal OM biopsy, given the heterogeneity of histopathology in healthy controls. Holbrook et al. reported that in a population of patients with various disease histories and controls, axon bundle integrity was more closely associated with olfactory performance than was OE integrity.[27] The current study focused on determining whether morphological and cytological patterns of the OE might relate to disease status and olfactory function within a group of well-characterized CRS patients and gaining a better understanding of the inflammatory process in the human OM.

Normal OMP-ir OSNs were detected in 45% of control biopsies, which is in agreement with previous studies demonstrating that approximately 50% of the biopsies from the high middle turbinate and apposing septum yield odorant-responsive OSNs as evidenced by calcium imaging[18], and 54% of such biopsies as determined by cytological assessment. [17] Although normal OMP-ir OSNs were detected in only 24% of CRS biopsies, this was not due to a lack of sensory epithelium, since morphologically abnormal OMP-ir and PGP9.5-ir OSNs were observed scattered throughout the OE of the remaining CRS biopsies, consistent with other reports.[27, 52, 53] Our immunohistochemical experiments also revealed OMP-ir cells with no PGP9.5 labeling. PGP9.5 or UCHL1 is a de-ubiquitinating enzyme needed for protein degradation and oxidative modification and a reduction in levels has been reported in neurodegenerative diseases that impact olfactory function, such as Parkinson's and Alzheimer's.[54] It may be that these mature OMP-ir OSNs are in the process of degeneration and consequently have lower levels of UCHL1 expression. Additional examination with biomakers for cell death will be needed to further characterize these neurons.

Analysis of the different OE morphological types revealed a significantly lower percentage of normal OE in CRS biopsies relative to control biopsies, suggesting that a loss of normal OE (sensorineural damage) and associated reduction in mature OSNs may play a role in secondary olfactory loss in CRS. The similar prevalences of goblet/intermixed OE in control and CRS biopsies suggest that this morphology may be normally present at the level of the upper middle turbinate and may be due to the proximity of the biopsied area to RE or to epithelial injury not specific to CRS, since damaged OE may be replaced with RE.[14]

Squamous metaplasia is the typical response of epithelia to injury, chemical irritation, or bacterial infection.[13] Calderon-Garciduenas and colleagues reported that local inflammation and accompanying high incidences of squamous metaplasia, basal cell hyperplasia, and neo-vascularization in the anterior middle turbinate were found in healthy volunteers, presumably due to their living in the polluted environment of Mexico City.[55] Hence the presence of squamous OE with abnormal OSNs in our control biopsies confirms that squamous transformation can occur in the OE of the middle turbinate of healthy subjects. In addition, the presence of both immature and mature OSNs indicates that neurogenesis is able to persist within squamous OE.

While the percentages of squamous OE are similar in CRS and control biopsies (Table 2), severe squamous metaplasia, defined qualitatively, was only observed in CRS biopsies.

Further characterization of keratinization patterns will be needed to define the nature and severity of squamous metaplasia in this tissue. The absence of OMP-ir in severe squamous OE that contained PGP9.5-ir-OSNs is similar to what has been reported in hyposmic patients with Parkinson's or other conditions.[53] This suggests that squamous transformation leads to cellular alterations that may hinder neuronal maturation and block the expression of OMP protein in OSNs or these neurons are phenotypically abnormal mature cells that nonetheless express other neuronal markers.

Squamous transformation also leads to the loss of olfactory sustentacular cells. These cells contain cytochrome P450s that play an important role in the metabolism of air-borne compounds found in the environment, providing protection for the underlying OSNs[50], as well as components of retinoid processing (i.e., retinaldehyde deydrogenase and cellular retinoic acid binding protein)[56] that may facilitate the differentiation of OSNs.[57] Hyperproliferation was also observed in squamous OE and is similar to what is seen after blocking sensory input via nasal occlusion.[58] The loss of OSN function due to structural impedance is associated with an increased neuronal turnover rate and cellular proliferation. Squamous layers may also serve as a layer of protection against further external insult to the underlining sensory epithelium, allowing cellular proliferation, differentiation and potential recovery to occur. [59]

Eroded OE was most prevalent in CRS anosmics, who also exhibited the highest density of eosinophils infiltrating the OE. Eosinophils release degradative enzymes (e.g., major basic protein) that compromise the cellular matrix and damage epithelial integrity[60], which could lead to a greater susceptibility to damage from daily exposure to environmental factors and to mechanical stresses, as encountered during the biopsy procedure. Inflammation also affects matrix metalloproteinases to alter intracellular composition of the extracellular matrix and induce changes in nasal tissue in both CRS and nasal polyposis.[61–63] It is possible that the 8% eroded OE observed in control biopsies occurred during surgical removal or tissue processing. However, some of the control biopsies with eroded OE had high densities of infiltrating immune cells, indicating that epithelial integrity may have been compromised due to local tissue inflammation unrelated to any clinical pathology.

The OE morphological heterogeneity in control biopsies may reflect a robust immune response to environmental irritants in healthy nasal tissue. In contrast, the more homogeneous OE profile observed in CRS biopsies may be due either to the persistent chronic inflammation characteristic of the disease or to local or systemic inflammatory responses to various treatments (e.g., corticosteroids and nasal sprays) received prior to study entry. Examination of multiple biopsies from other regions of the OM will be needed to determine if the observed degree of anatomical and cellular alterations in the middle turbinate of CRS patients is characteristic of the OM as a whole. Nevertheless, these sensorineural changes do seem to reflect the disease state of the OM in the CRS population, and we examined whether these observations were associated with particular sensory or clinical profiles in the CRS population.

Clinical assessments of our CRS patients with differing degrees of olfactory dysfunction were similar to those reported by Litvack et al., who assessed possible predictors of

olfactory dysfunction in a large CRS group (>350 patients).[64, 65] The prevalence of hyposmia and anosmia among our patients was 13.2% and 11.5% lower, respectively, than observed in their study, perhaps due in part to our exclusion of patients over 60 years of age. However, as Litvack et al. also reported, we found associations between olfactory dysfunction and nasal polyposis, endoscopy scores and CT scores but not many other subject characteristics, such as allergic rhinitis or prior sinus surgery.

The presence of normal OMP-ir OSNs in CRS hyposmics (57.2% of biopsies), although somewhat lower than in normosmic patients (73.4% of biopsies), suggests that olfactory dysfunction in hyposmic CRS patients may be primarily related to conductive factors. A more selective grouping of these CRS hyposmics based on more detailed clinical and inflammatory assessments (e.g., measures of nasal airflow and cytokine levels) may help to clarify to what extent conductive and sensorineural factors contribute to their olfactory dysfunction.

Our analysis of the CRS anosmic group suggests that multiple conductive and sensorineural factors contribute to olfactory loss in these patients. Only two biopsies in the anosmic group had OMP-ir OSNs and both were diagnosed with marked polyposis. While a visible airway was seen along the inferior nasal cavity in both patients, airflow to and odorant deposition in the olfactory cleft was likely to be severely restricted. The remaining three anosmics received diagnoses of polyposis that ranged from early to severe, but their biopsies showed either >50% eroded OE or 100% squamous OE and an absence of normal OMP-ir OSNs. A loss of mature OSNs might play a greater role in smell loss in these patients than in that of the other two patients. Recovery of olfaction might be less likely or delayed even subsequent to surgical polypectomy, in view of the evident need for more extensive regeneration of the OE. However, OE in the upper recesses of the nasal cavity might be less affected by polyposis and epithelial erosion. Our overall assessments of anosmic CRS patients yielded findings similar to previous studies[22] in which complete smell loss has been strongly associated with nasal polyposis.

An interesting finding from this study is the significantly shorter duration of CRS-related symptoms reported in the CRS anosmics. We hypothesize that epithelial erosion due to high eosinophilic infiltration, perhaps associated with more virulent bacterial, fungal or viral upper respiratory infections in some patients, may occur during the early stages of the disease. With continued inflammation, the presence of squamous metaplasia and goblet cell hyperplasia may reflect epithelial recovery leading to cellular repair of the OM. Inflammation and its impact on the OM clearly fluctuates across the sensory epithelial sheet; hence a complete understanding of the temporal development of OM pathology in CRS will require a means to sample multiple OM sites and time points within an individual.

Our detailed examination of the nasal biopsies revealed a variety of distinct epithelial morphologies that can affect olfactory neurogenesis, differentiation and maturation of OSNs in the human OM. Our results demonstrate that the loss of mature OSNs due to eosinophilic infiltration is likely to play a significant role in at least some cases of olfactory disability in CRS. While biopsy size may limit the degree to which correlations can be made between tissue pathology and sensory ability, the comprehensive cytological and morphological

analyses presented provide an important snapshot into the dynamic processes of epithelial injury/repair that occur throughout life in this regenerative tissue.

## Acknowledgments

We appreciate all of our CRS patients and control subjects who volunteered tissue for this study. We thank Dr. Moira Woods for her expertise in understanding nasal histopathology and Dr. Anne-Marie Galioto and Ryan Moore for their assistance in the initial stages of this study. We acknowledge lab members, Dr. Martin Witt and Dr. Eric Holbrook for their helpful discussions and thank Dr. Joe Brand for reviewing this manuscript. Finally, we appreciate the helpful comments and suggestions made by two anonymous reviewers on improving this manuscript.

Supported by the National Institute on Deafness and Other Communication Disorders DC006760 (G.K. Beauchamp) and National Science Foundation DBI-0216310 (NER) and by National Institute of Mental Health MH-08193 (CGH).

## References

1. Cowart BJ, Young IM, Feldman RS, et al. Clinical disorders of smell and taste. Occup Med. 1997; 12:465–483. [PubMed: 9298495]
2. Blackwell DL, Collins JG, Coles R. Summary health statistics for U.S. adults: National Health Interview Survey, 1997. Vital Health Stat 10. 2002:1–109.
3. Benninger MS, Ferguson BJ, Hadley JA, et al. Adult chronic rhinosinusitis: definitions, diagnosis, epidemiology, and pathophysiology. Otolaryngol Head Neck Surg. 2003; 129:S1–32. [PubMed: 12958561]
4. Meltzer EO, Hamilos DL, Hadley JA, et al. Rhinosinusitis: establishing definitions for clinical research and patient care. J Allergy Clin Immunol. 2004; 114:155–212. [PubMed: 15577865]
5. Loury, MC., Kennedy, DW. Chronic Sinusitis and Nasal Polyposis. In: Getchell, TV.Bartoshuk, LM.Doty, RL., et al., editors. Smell and Taste in Health and Disease. New York: Raven Press; 1991. p. 517-528.
6. Raviv JR, Kern RC. Chronic rhinosinusitis and olfactory dysfunction. 2006:108–124.
7. Snow, JB, Jr. Causes of olfactory and gustatory disorders. In: Getchell, TV.Bartoshuk, LM.Doty, RL., et al., editors. Smell and Taste in Health and Disease. New York: Raven Press; 1991. p. 445-449.
8. Farbman, AI. Cell Biology of Olfaction. New York: Cambridge University Press; 1991.
9. Gilad Y, Lancet D. Population differences in the human functional olfactory repertoire. Mol Biol Evol. 2003; 20:307–314. [PubMed: 12644552]
10. Restrepo D, Teeter JH, Schild D. Second messenger signaling in olfactory transduction. J Neurobiol. 1996; 30:37–48. [PubMed: 8727981]
11. Shipley MT, Ennis M. Functional organization of olfactory system. J Neurobiol. 1996; 30:123–176. [PubMed: 8727988]
12. Graziadei PPC, Monti Graziadei GA. Neurogenesis and neuron regeneration in the olfactory system of mammals. I. Morphological aspects of differentiation and structural organization of the olfactory sensory neurons. J Neurocytol. 1979; 8:1–18. [PubMed: 438867]
13. Harkema JR, Carey SA, Wagner JG. The nose revisited: a brief review of the comparative structure, function, and toxicologic pathology of the nasal epithelium. Toxicol Pathol. 2006; 34:252–269. [PubMed: 16698724]
14. Morrison EE, Costanzo RM. Morphology of the human olfactory epithelium. J Comp Neurol. 1990; 297:1–13. [PubMed: 2376627]
15. Paik SI, Lehman MN, Seiden AM, et al. Human olfactory biopsy. The influence of age and receptor distribution. Arch Otolaryngol Head Neck Surg. 1992; 118:731–738. [PubMed: 1627295]
16. Leopold DA, Hummel T, Schwob JE, et al. Anterior distribution of human olfactory epithelium. Laryngoscope. 2000; 110:417–421. [PubMed: 10718430]
17. Feron F, Perry C, McGrath JJ, et al. New techniques for biopsy and culture of human olfactory epithelial neurons. Arch Otolaryngol Head Neck Surg. 1998; 124:861–866. [PubMed: 9708710]

18. Rawson NE, Gomez G, Cowart B, et al. Selectivity and response characteristics of human olfactory neurons. J Neurophysiol. 1997; 77:1606–1613. [PubMed: 9084623]
19. Nakashima T, Kimmelman CP, Snow JB Jr. Structure of human fetal and adult olfactory neuroepithelium. Arch Otolaryngol. 1984; 110:641–646. [PubMed: 6477257]
20. Milbrath MM, Madiedo GTRJ. Histopathological analysis of the middle turbinate after ethmoidectomy. Am J Rhinol. 1994; 8:37–42.
21. Goldwyn BG, Sakr W, Marks SC. Histopathological analysis of chronic sinusitis. Am J Rhinol. 1995; 9:27–30.
22. Van Zele T, Claeys S, Gevaert P, et al. Differentiation of chronic sinus diseases by measurement of inflammatory mediators. Allergy. 2006; 61:1280–1289. [PubMed: 17002703]
23. Rehl RM, Balla AA, Cabay RJ, et al. Mucosal remodeling in chronic rhinosinusitis. Am J Rhinol. 2007; 21:651–657. [PubMed: 18201442]
24. Baudoin T, Kalogjera L, Geber G, et al. Correlation of histopathology and symptoms in allergic and non-allergic patients with chronic rhinosinusitis. Eur Arch Otorhinolaryngol. 2008; 265:657–661. [PubMed: 18004580]
25. Soler ZM, Sauer DA, Mace J, et al. Relationship between clinical measures and histopathologic findings in chronic rhinosinusitis. Otolaryngol Head Neck Surg. 2009; 141:454–461. [PubMed: 19786212]
26. Kern RC. Chronic sinusitis and anosmia: pathologic changes in the olfactory mucosa. Laryngoscope. 2000; 110:1071–1077. [PubMed: 10892672]
27. Holbrook EH, Leopold DA, Schwob JE. Abnormalities of axon growth in human olfactory mucosa. Laryngoscope. 2005; 115:2144–2154. [PubMed: 16369158]
28. Feng P, Yee KK, Cowart BJ, et al. Immune cell profile in the olfactory epithelium of patients with chronic nasal inflammation. Chem Senses. 2007; 32:A28.
29. Galioto A, Yee KK, Ozdener H, et al. The impact of inflammation on the olfactory epithelium in patients with chronic rhinosinusitis. Chem Senses. 2005; 30:A210.
30. Yee KK, Ozdener H, Cowart BJ, et al. Neuronal and inflammatory changes in nasal tissues of chronic rhinosinusitis patients. Chem Senses. 2006; 31:A5.
31. Yee KK, Cowart BJ, Pribitkin EA, et al. Role of cytochrome P450 in the nasal inflammatory process. Chem Senses. 2007; 32:A27.
32. Yee KK, Feng P, Pribitkin EA, et al. Analysis of the olfactory mucosa in chronic rhinosinusitis. Ann N Y Acad Sci. 2009; 1170:590–595. [PubMed: 19686198]
33. Lehman DA, Casiano RR, Polak M. Reliability of the University of Miami chronic rhinosinusitis staging system. Am J Rhinol. 2006; 20:11–19. [PubMed: 16539288]
34. Doty RL, Brugger WE, Jurs PC, et al. Intranasal trigeminal stimulation from odorous volatiles: psychometric responses from anosmic and normal humans. Physiol Behav. 1978; 20:175–185. [PubMed: 662939]
35. Kobal, G. A new methold for determination of the olfactory and the trigeminal nerve's dysfunction: olfactory (OEP) and chemical somatosensory (CSEP) evoked potentials. In: Rothenberger, A., editor. Event-Related Potentials in Children. Amsterdam: Elsevier Biomedical Press; 1982. p. 455-461.
36. Wysocki CJ, Cowart BJ, Radil T. Nasal trigeminal chemosensitivity across the adult life span. Percept Psychophys. 2003; 65:115–122. [PubMed: 12699314]
37. Weatherill GG, Leavitt H. Sequential estimation of points on a psychometric function. Fr J Math Statis Psycol. 1965; 18:1–10.
38. Pribitkin E, Rosenthal MD, Cowart BJ. Prevalence and causes of severe taste loss in a chemosensory clinic population. Ann Otol Rhinol Laryngol. 2003; 112:971–978. [PubMed: 14653367]
39. Cowart BJ, Flynn-Rodden K, McGeady SJ, et al. Hyposmia in allergic rhinitis. J Allergy Clin Immunol. 1993; 91:747–751. [PubMed: 8454797]
40. Lowry, LD., Pribitkin, EA. Collection of human olfactory biopsy. In: Spielman, AI., Brand, JG., editors. Experimental Cell Biology of Taste and Olfaction. Boca Raton, FL: CRS; 1995. p. 47-48.

41. Keller A, Margolis FL. Immunological studies of the rat olfactory marker protein. J Neurochem. 1975; 24:1101–1106. [PubMed: 805214]
42. Wilkinson KD, Lee KM, Deshpande S, et al. The neuron-specific protein PGP 9.5 is a ubiquitin carboxyl-terminal hydrolase. Science. 1989; 246:670–673. [PubMed: 2530630]
43. Weiler E, Benali A. Olfactory epithelia differentially express neuronal markers. J Neurocytol. 2005; 34:217–240. [PubMed: 16841165]
44. Verhaagen J, Oestreicher AB, Gispen WH, et al. The expression of the growth associated protein B50/GAP43 in the olfactory system of neonatal and adult rats. J Neurosci. 1989; 9:683–691. [PubMed: 2918383]
45. Lee MK, Rebhun LI, Frankfurter A. Posttranslational modification of class III beta-tubulin. Proc Natl Acad Sci U S A. 1990; 87:7195–7199. [PubMed: 2402501]
46. Roskams AJ, Cai X, Ronnett GV. Expression of neuron-specific beta-III tubulin during olfactory neurogenesis in the embryonic and adult rat. Neuroscience. 1998; 83:191–200. [PubMed: 9466409]
47. Hahn CG, Han LY, Rawson NE, et al. In vivo and in vitro neurogenesis in human olfactory epithelium. J Comp Neurol. 2005; 483:154–163. [PubMed: 15678478]
48. Suzuki Y, Takeda M. Keratins in the developing olfactory epithelia. Brain Res Dev Brain Res. 1991; 59:171–178. [PubMed: 1717178]
49. Williams SK, Gilbey T, Barnett SC. Immunohistochemical studies of the cellular changes in the peripheral olfactory system after zinc sulfate nasal irrigation. Neurochem Res. 2004; 29:891–901. [PubMed: 15139288]
50. Chen Y, Liu YQ, Su T, et al. Immunoblot analysis and immunohistochemical characterization of CYP2A expression in human olfactory mucosa. Biochem Pharmacol. 2003; 66:1245–1251. [PubMed: 14505803]
51. Winer, BJ. Statistical principals in experimental design. New York: McGraw-Hill; 1971.
52. Lane AP, Gomez G, Dankulich T, et al. The superior turbinate as a source of functional human olfactory receptor neurons. Laryngoscope. 2002; 112:1183–1189. [PubMed: 12169895]
53. Witt M, Bormann K, Gudziol V, et al. Biopsies of olfactory epithelium in patients with Parkinson's disease. Mov Disord. 2009; 24:906–914. [PubMed: 19205070]
54. Setsuie R, Wada K. The functions of UCH-L1 and its relation to neurodegenerative diseases. Neurochem Int. 2007; 51:105–111. [PubMed: 17586089]
55. Calderon-Garciduenas L, Rodriguez-Alcaraz A, Villarreal-Calderon A, et al. Nasal epithelium as a sentinel for airborne environmental pollution. Toxicol Sci. 1998; 46:352–364. [PubMed: 10048139]
56. Asson-Batres MA, Smith WB. Localization of retinaldehyde dehydrogenases and retinoid binding proteins to sustentacular cells, glia, Bowman's gland cells, and stroma: potential sites of retinoic acid synthesis in the postnatal rat olfactory organ. J Comp Neurol. 2006; 496:149–171. [PubMed: 16538685]
57. Hagglund M, Berghard A, Strotmann J, et al. Retinoic acid receptor-dependent survival of olfactory sensory neurons in postnatal and adult mice. J Neurosci. 2006; 26:3281–3291. [PubMed: 16554478]
58. Farbman AI, Brunjes PC, Rentfro L, et al. The effect of unilateral naris occlusion on cell dynamics in the developing rat olfactory epithelium. J Neurosci. 1988; 8:3290–3295. [PubMed: 2459323]
59. Yee KK, Pribitkin EA, Cowart BJ, et al. Smoking-associated Squamous Metaplasia in Olfactory Mucosa of Patients With Chronic Rhinosinusitis. Toxicol Pathol. 2009; 37:594–598. [PubMed: 19487255]
60. Ponikau JU, Sherris DA, Kephart GM, et al. Features of airway remodeling and eosinophilic inflammation in chronic rhinosinusitis: is the histopathology similar to asthma? J Allergy Clin Immunol. 2003; 112:877–882. [PubMed: 14610473]
61. Watelet JB, Bachert C, Claeys C, et al. Matrix metalloproteinases MMP-7, MMP-9 and their tissue inhibitor TIMP-1: expression in chronic sinusitis vs nasal polyposis. Allergy. 2004; 59:54–60. [PubMed: 14674934]

62. Chen YS, Langhammer T, Westhofen M, et al. Relationship between matrix metalloproteinases MMP-2, MMP-9, tissue inhibitor of matrix metalloproteinases-1 and IL-5, IL-8 in nasal polyps. Allergy. 2007; 62:66–72. [PubMed: 17156344]

63. Kostamo K, Tervahartiala T, Sorsa T, et al. Metalloproteinase function in chronic rhinosinusitis with nasal polyposis. Laryngoscope. 2007; 117:638–643. [PubMed: 17429873]

64. Litvack JR, Fong K, Mace J, et al. Predictors of olfactory dysfunction in patients with chronic rhinosinusitis. Laryngoscope. 2008; 118:2225–2230. [PubMed: 19029858]

65. Litvack JR, Mace JC, Smith TL. Olfactory function and disease severity in chronic rhinosinusitis. Am J Rhinol Allergy. 2009; 23:139–144. [PubMed: 19401037]

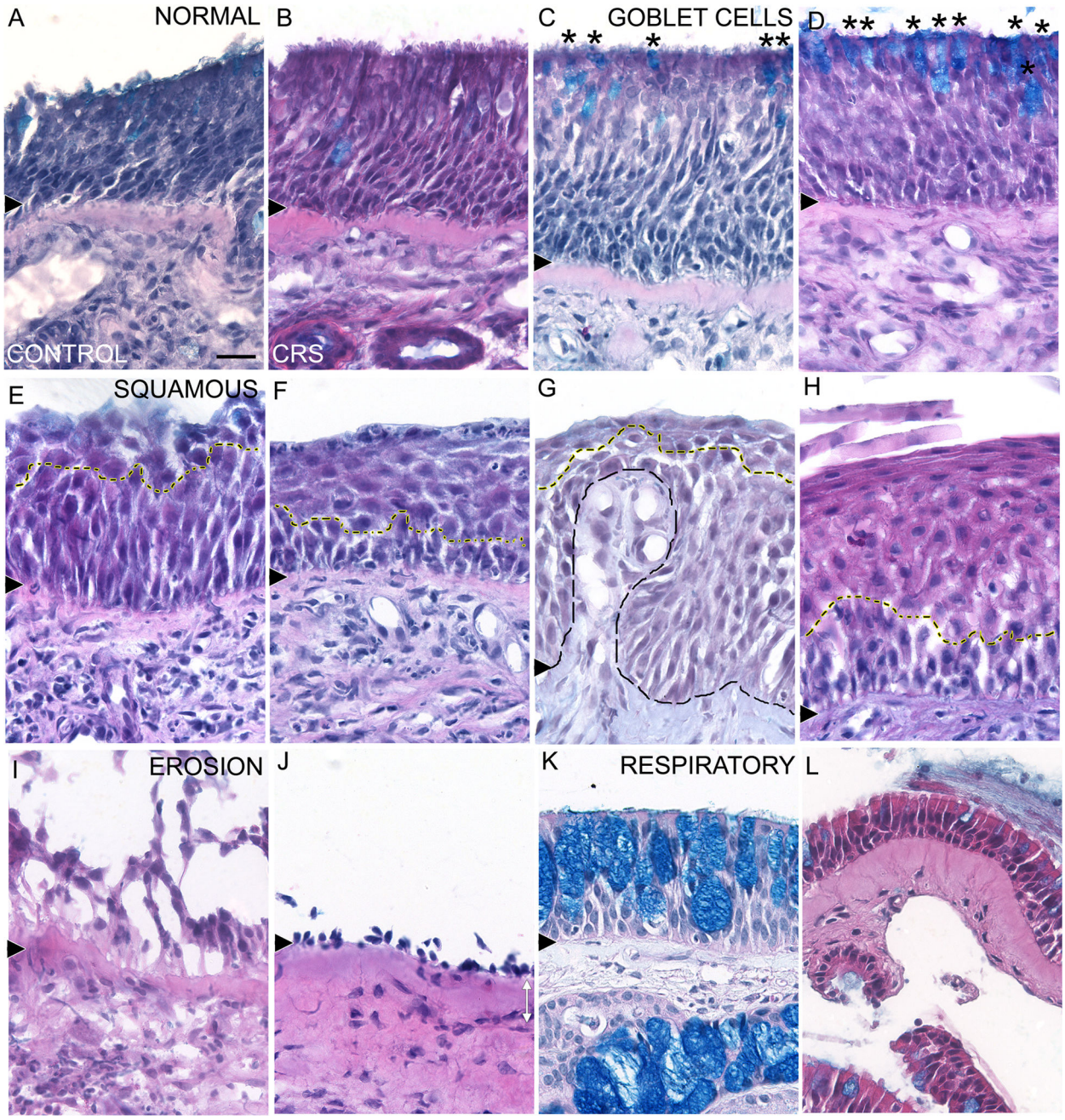


**Figure 1. Epithelial Morphologies of Control and CRS Nasal Biopsies**

A – B. Normal pseudostratified sensory epithelium was present in control (A) and CRS biopsies (B). C – D. Intermixing of Alcian Blue-stained goblet cells (asterisks) in normal pseudostratified epithelium was observed in the control (C) and CRS biopsies (D). E – H. Examples of varying degrees of epithelial transformation into squamous layers. Mild squamous metaplasia with a few layers of cuboid-shaped squamous-like cells (yellow dashed line, E) and moderate squamous metaplasia with a thicker layer of distinctive squamous-like cells (yellow dashed line, F) were observed in control biopsies. Invaginations of lamina propria (black dashed line) into mild squamous metaplasia (yellow dashed line)

were often observed in CRS biopsies (G). More severe squamous metaplasia composed of several layers of distinctive squamous-like cells and flattened cells at the apical surface (yellow dashed line) was also frequently observed in CRS biopsies (H). I – J. Reduction in or loss of epithelial integrity led to erosion of cellular layers in both control (I) and CRS biopsies (J). K – L. Respiratory epithelium was identified either by a high density of Alcian Blue-stained goblet cells in the epithelium (K) or thin epithelial layers. Note also the Alcian Blue-stained mucus cells in the lamina propria. Black arrowhead = basement membrane. Scale bar = 20μm.

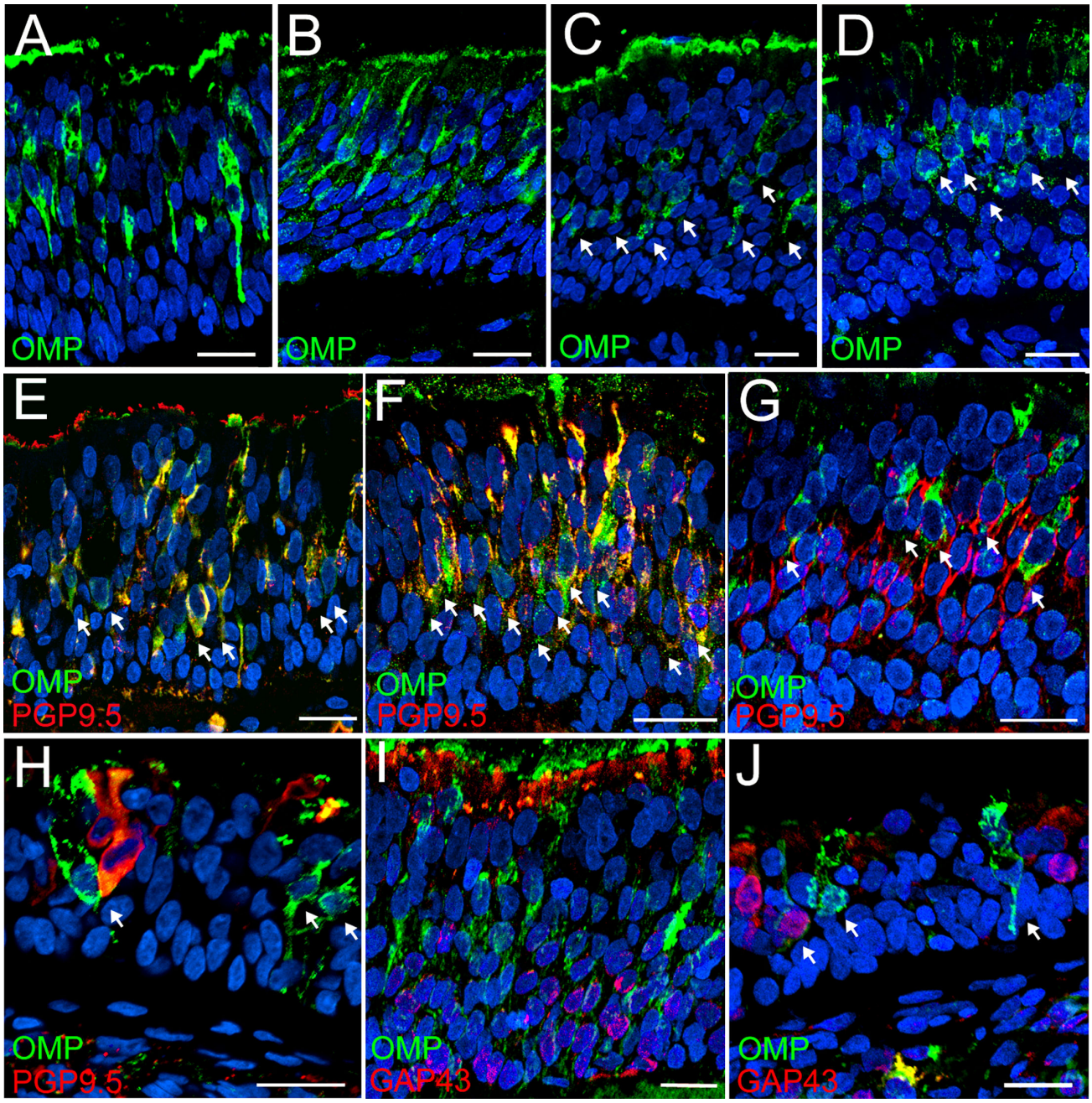


**Figure 2. Immunohistochemical Labeling of Olfactory Sensory Neurons**

A–D. Bipolar mature OMP-ir OSNs (green) were found in the middle layers of the normal pseudostratified OE of control (A) and CRS biopsies (B). OMP-ir OSNs (green, arrows) were also observed in goblet/intermixed OE of control (C) and CRS biopsies (D) though with less distinguishable OMP labeled processes. To further demonstrate the presence of sensory epithelium in our nasal biopsies, the OE regions in Fig 2A–D correspond to the OE region in Fig 1A–D. E–H. Double immunofluorescence labeling with OMP and PGP9.5 found the expression of these neuronal proteins varied in mature OSNs. OMP-ir cells (green, arrows) were labeled with PGP9.5 (red), especially in the processes (E–F). In other OE

region of the same control biopsy, a few OMP-ir cells with PGP9.5 labeled processes were observed among PGP-ir cells (G). In an OE region with scattered neurons, a few OMP-ir cells with no PGP9.5 labeling were observed (arrows, H). I–J. Layers of immature GAP-ir cells (red) were observed below mature OMP-ir OSNs (green) suggesting olfactory neurogenesis is still on-going in these biopsies. Blue = DAPI. Scale bar = 20μm.

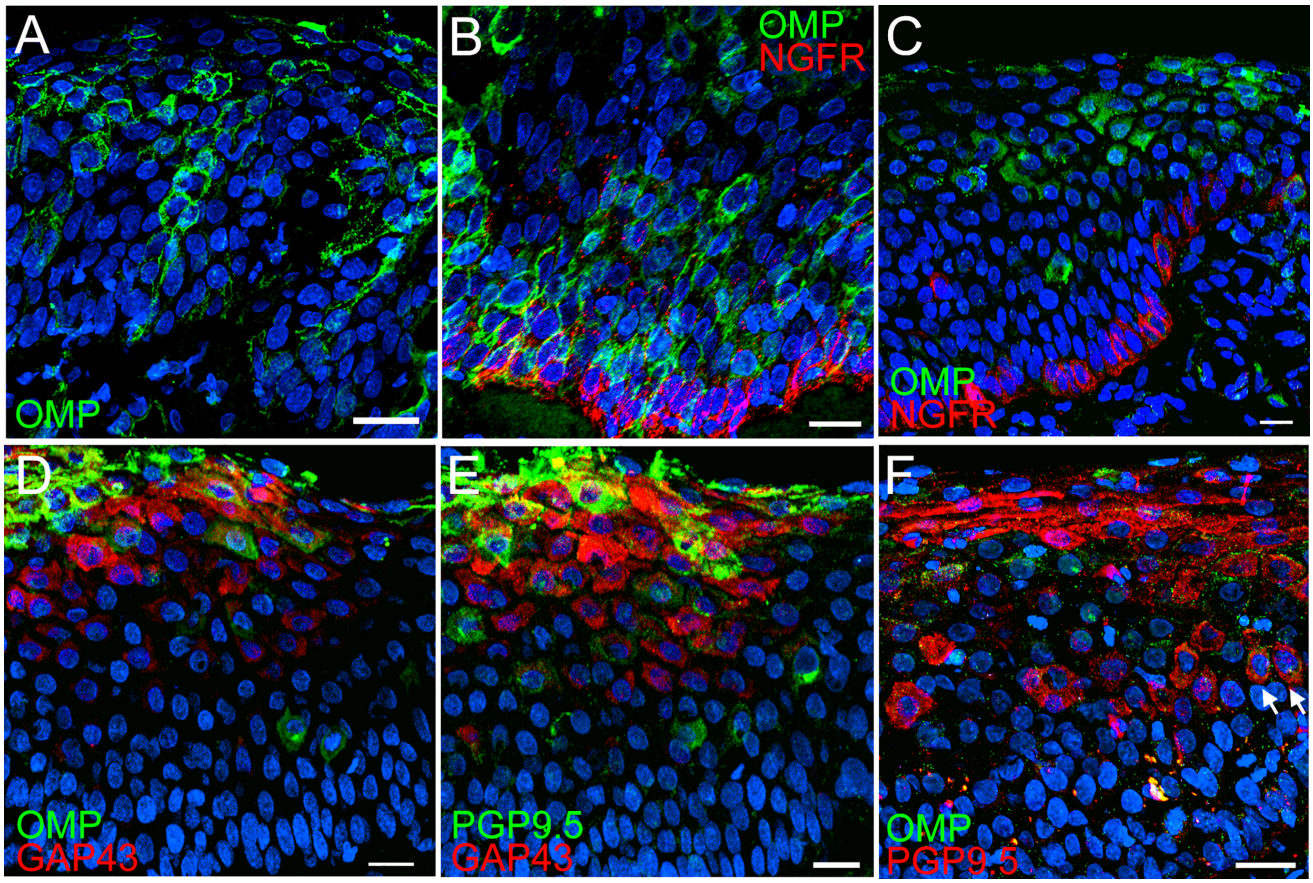


**Figure 3. Immunohistochemical Labeling of Neuronal Cells in Squamous Olfactory Epithelium**

A–B. Mild squamous metaplasia disrupted the localization of OMP-ir OSNs (green) such that OSNs were observed at all cellular layers (A) and localized in layers just above NGFR-ir basal cells (red, B). The OE region in 3A corresponds to Fig 1G. C–E. In moderate squamous metaplasia, mature OMP-ir OSNs (green) become abnormally shape and scattered (C) and immature GAP43-ir cells (red) were observed with OMP-ir cells (green, D), suggesting neurogenesis is still present after squamous transformation. In adjacent sections of the same CRS biopsy, a few GAP43-ir cells (red) were also labeled weakly with PGP (green, E). F. In a biopsy with severe squamous OE, only a few abnormally shaped PGP-ir cells (red) with weak OMP-ir (green, arrows) were observed. Non-specific immunoreactivity was observed in the apical flat cells. This OE region corresponds to Fig 1H. Blue = DAPI. Scale bar = 20μm.

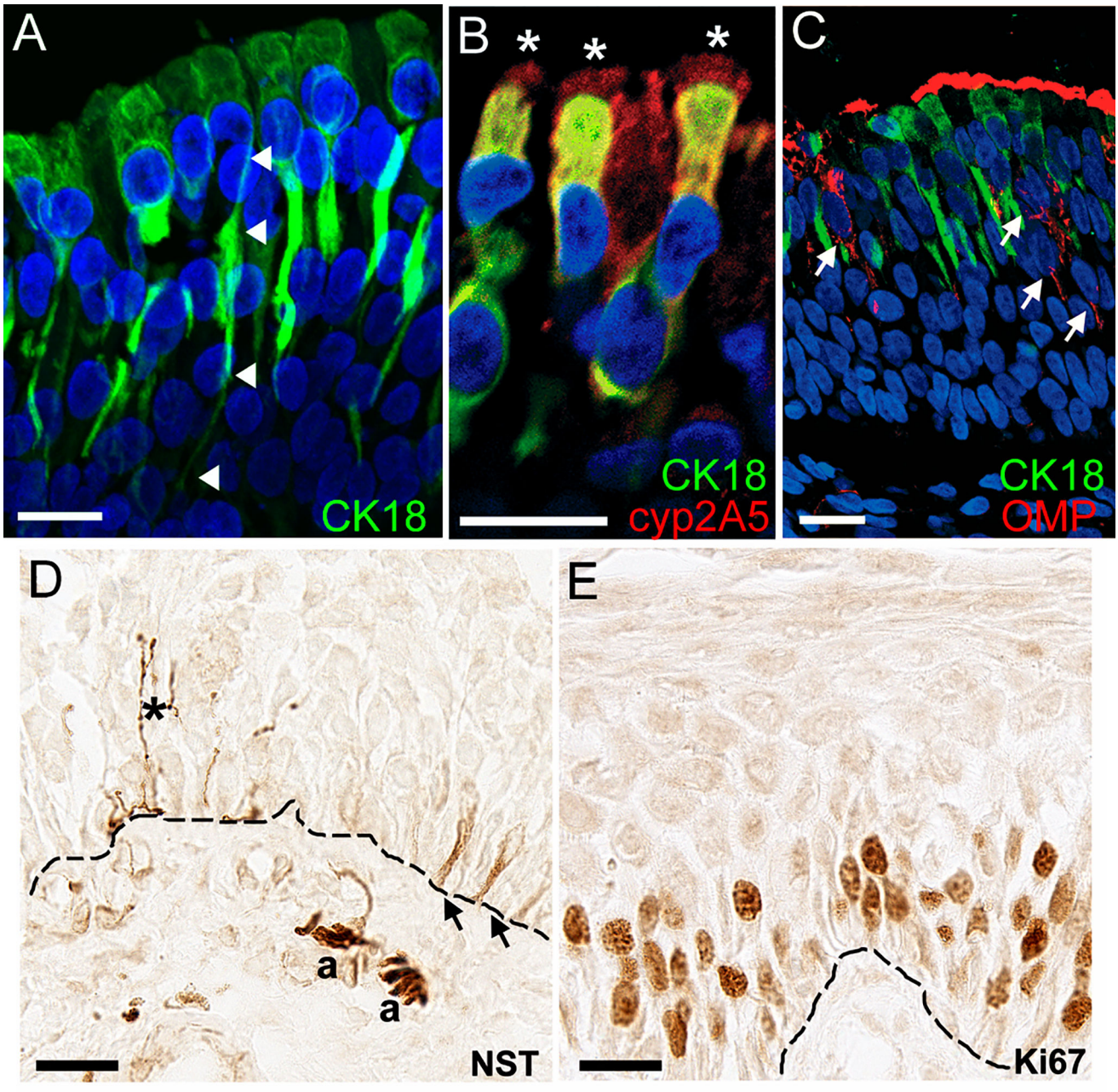


**Figure 4. Immunhistochemical Evaluation of the Cellular Profile in Control and CRS Nasal Biopsies**

A. CK18-ir olfactory sustentacular cells (green) were located in the apical layers of the OE. Arrowheads indicate a characteristic olfactory sustentacular cell with process extending to the basement membrane. CK18-ir was also observed in Bowman's glands and mucus glands (data not shown). B. Cyp2A5-ir (red) was co-localized in CK18-ir olfactory sustentacular cells (green) with prominent cyp2A5-ir in the cilia (asterisks). C. The presence of OMP-ir OSNs (red) among CK18-ir olfactory sustentacular cells (green) indicates CK18-ir may assist in identifying areas of sensory epithelium. D. NST-ir was seen in trigeminal fibers extending into the OE (asterisk), cells at the basal layer (arrows), and small nerve bundles

(a) in the lamina propria. E. The presence of numerous proliferating Ki67-ir cells was characteristic of squamous OE. Blue = DAPI. Basement membrane = dashed line. Scale bar = 20μm.

## Table 1

Antibody list.

| Antibody | Cat Num | Clone | Dilution | Cell Type |
|---|---|---|---|---|
| β-tubulin III | MMS-435P | TUJ1 | 1:500/1:250 F | axons, trigeminal fibers |
| CK18 | MAB3234 | RGE53 | 1:1000/1:500 F | supporting cells, mucus glands |
| Cytochrome 2A5 | Dr. X. Ding | | 1:500/1:250 F | supporting cells, mucus glands |
| GAP43 | 69264 | | 1:1000/1:500 F | immature OSNs |
| Ki67 | RB-081-A3 | | 1:1000/1:500 F | proliferating cells |
| p75 NGFR | MAB5386 | ME20.4 | 1:500/1:250 F | basal cells |
| OMP | 54-1000 | 3F151 | 1:2000/1:1000 F | mature OSNs |
| PGP9.5 | AB1761 | | 1:2000/1:500 F | neuronal cells |
| Elastase | E2230 | | 1:200 | Neutrophils |
| CD64 | 555525 | 10.1 | 1:50 | Macrophages |
| Major Basic Protein (MBP) | 550843 | | 1:50 | Eosinophils |

## Table 2

Quantitative analyses of control and CRS biopsies.

| | CONTROL n = 20 | CRS n = 50 |
|---|---|---|
| ***OE MORPHOLOGY*** | | |
| **normal (%OE)** | 23.04 ± 4.69 | 12.01 ± 2.39 * |
| **goblet intermixed (%OE)** | 33.44 ± 7.50 | 39.37 ± 4.37 |
| **squamous (%OE)** | 35.97 ± 7.36 | 33.41 ± 5.14 |
| **erosion (%OE)** | 8.08 ± 2.69 | 15.40 ± 3.73 |
| ***OM MEASUREMENTS*** | | |
| **OMP-ir OSNs †, N biopsies (%)** | 9 (45.0) | 12 (24.0) |
| **OE thickness (μm)** | 66.29 ± 5.41 | 62.68 ± 4.15 |
| **BM thickness (μm)** | 13.53 ± 1.04 | 12.89 ± 0.81 |
| **BV density (#/200μm$^2$)** | 3.90 ± 0.42 | 4.29 ± 0.29 |
| **MG density (#/200μm$^2$)** | 3.49 ± 0.73 | 4.36 ± 0.42 |
| ***IMMUNE CELLS*** | | |
| **eosinophils (#/mm OE)** | 0.38 ± 0.16 | 1.96 ± 0.57 |
| **macrophages (#/mm OE)** | 25.95 ± 6.32 | 13.88 ± 2.79 * |
| **neutrophils (#/mm OE)** | 36.85 ± 12.90 | 19.68 ± 4.07 |

± standard error

* p value ≤ 0.05

† = differences between groups in the number of biopsies with normal OMP-ir OSNs were analyzed using Fisher's exact test; all other comparisons are by t-test.

BM = basement membrane; BV = blood vessel; MG = mucus gland; OE = olfactory epithelium; OMP-ir = olfactory marker protein immunoreactivity; OSNs = olfactory sensory neurons.

**Table 3**

Quantitative analyses based on predominant epithelial histopathology for control and CRS biopsies.

| | CON-NORM* n = 2 | CON-GB n = 9 | CON-SQ n = 9 | CRS-GB n =23 | CRS-SQ n = 21 | CRS-ER n = 6 |
|---|---|---|---|---|---|---|
| ***OE MORPHOLOGY*** | | | | | | |
| **normal (%OE)** | 66.65 ± 5.15 | 18.21 ± 5.09[a] | 18.17 ± 5.53[a] | 18.68 ± 4.12[a] | 7.70 ± 2.79[b] | 1.52 ± 1.52[b] |
| **goblet intermixed (%OE)** | 22.38 ± 5.78 | 63.65 ± 8.60[a] | 5.09 ± 2.88[b] | 65.32 ± 4.59[a] | 17.22 ± 3.54[b] | 17.37 ± 8.54[b] |
| **squamous (%OE)** | 0.00 | 12.76 ± 5.17[a] | 67.18 ± 5.87[b] | 6.78 ± 2.44[a] | 71.22 ± 4.78[b] | 3.17 ± 3.17[a] |
| **erosion (%OE)** | 10.95 ± 10.95 | 5.28 ± 2.17[a] | 10.23 ± 5.3[a] | 9.20 ± 2.73[a] | 4.33 ± 2.09[a] | 77.95 ± 7.13[b] |
| ***OM MEASUREMENTS*** | | | | | | |
| **OMP-ir OSNs†, N biopsies (%)** | 2 (100) | 5 (55.6)[a] | 2 (22.2)[ab] | 12 (52.2)[a] | 0 (0.0)[b] | 0 (0.0)[b] |
| **OE thickness (μm)** | 47.05 ± 14.91 | 59.16 ± 6.58[a] | 77.62 ± 8.49[a] | 63.44 ± 4.90[a] | 72.52 ± 6.56[a] | 25.26 ± 6.81[b] |
| **BM thickness (μm)** | 8.74 ± 1.40 | 13.33 ± 1.43 | 14.79 ± 1.65 | 13.24 ± 0.98 | 12.74 ± 1.45 | 12.06 ± 2.78 |
| **BV density (#/200μm$^2$)** | 2.17 ± 1.06 | 3.15 ± 0.55[a] | 5.04 ± .053[b] | 3.58 ± 0.39[a] | 5.19 ± 0.44[b] | 3.88 ± 0.67[ab] |
| **MG density (#/200μm$^2$)** | 7.83 ± 2.61 | 3.85 ± 1.19 | 2.17 ± 0.67 | 5.29 ± 0.51 | 3.34 ± 0.57 | 4.36 ± 1.97 |
| ***IMMUNE CELLS*** | | | | | | |
| **eosinophils (#/mm$^2$ OE)** | 1.23 ± 1.23 | 0.30 ± 0.23[a] | 0.26 ± 0.14[a] | 0.53 ± 0.23[a] | 2.39 ± .099[a] | 5.95 ± 2.72[b] |
| **macrophages (#/mm$^2$ OE)** | 7.84 ± 1.97 | 7.55 ± 2.36[ab] | 48.37 ± 9.53[c] | 6.08 ± 1.67[a] | 19.03 ± 3.40[ab] | 25.74 ± 18.30[b] |
| **neutrophils (#/mm$^2$ OE)** | 14.22 ± 14.22 | 5.87 ± 1.47[a] | 72.9 ± 23.96[b] | 11.42 ± 3.74[a] | 23.58 ± 5.31[a] | 37.72 ± 24.40[ab] |

*This group was not included in statistical analyses.

± standard error; non-overlapping letter superscripts reflect group differences at $p \leq 0.05$

†= differences in the number of biopsies with normal OMP-ir OSNs were analyzed using Fisher's exact tests; all other pairwise comparisons were by Fisher's LSD. In rows without letter superscripts, the main effect for group was not significant in the overall ANOVA.

ANOVA = analysis of variance; BM = basement membrane; BV = blood vessel; NORM = normal; GB = goblet cell; SQ = squamous; ER = erosion; MG = mucus gland; OE = olfactory epithelium; OMP-ir = olfactory marker protein immunoreactivity; OSNs = olfactory sensory neurons.

**Table 4**

Clinical Assessments and Morphological Comparison Based on Worst Olfactory Performance in CRS.

| | CONTROL n = 20 | CRS NORMOSMIC n = 29 | CRS HYPOSMIC n = 16 | CRS ANOSMIC n = 5 |
|---|---|---|---|---|
| **AGE** | 33.6 ± 2.54 | 41.66 ± 2.16 | 38.38 ± 3.49 | 45.6 ± 4.26 |
| **WORST PEA** | 10.41 ± 0.41[a] | 10.67 ± 0.40[a] | 5.66 ± 0.28[b] | 0.0[c] |
| **SMOKER†, N (%)** | 2 (10.0) | 4 (13.8) | 4 (25.0) | 0 (0.0) |
| **ALLERGY†, N (%)** | - | 8 (27.6) | 4 (25.0) | 1 (20.0) |
| **DURATION (yrs)** | - | 19.1 ± 2.68[a] | 12.0 ± 2.14[ab] | 3.4 ± 1.69[b] |
| ***SYMPTOMS*** | | | | |
| **congestion†, N (%)** | - | 26 (89.7) | 16 (100) | 5 (100) |
| **facial pain†, N (%)** | - | 24 (82.8) | 15 (93.8) | 3 (60.0) |
| **headaches†, N (%)** | - | 20 (69.0) | 12 (75.0) | 4 (80.0) |
| **post nasal drip†, N (%)** | - | 23 (79.3) | 11 (68.8) | 4 (80.0) |
| **runny nose†, N (%)** | - | 20 (69.0) | 10 (62.5) | 3 (60.0) |
| ***ENDOSCOPY‡*** | | | | |
| **diagnosed polyps†, N (%)** | - | 0 (0.0)[a] | 0 (0.0)[a] | 3 (60.0)[b] |
| **Early polyps†, N (%)** | - | 4 (13.8) | 3 (18.8) | 2 (40.0) |
| **Endoscore (avg)** | - | 4.31 ± 0.41[a] | 4.37 ± 0.68[a] | 11.2 ± 0.8[b] |
| ***CT STAGING‡*** | | | | |
| **anteth (avg)** | - | 1.61 ± 0.32[a] | 1.38 ± 0.41[a] | 6.4 ± 0.75[b] |
| **posteh (avg)** | - | 1.0 ± 0.29[a] | 0.63 ± 0.26[a] | 6.0 ± 1.1[b] |
| **ctscore (avg)** | - | 7.07 ± 1.00[a] | 6.81 ± 1.16[a] | 19.0 ± 1.54[b] |
| ***PRIOR NASAL SURGERY*** | | | | |
| **septum repair†, N (%)** | - | 2 (6.9) | 2 (12.5) | 0 (0.0) |
| **polypectomy†, N (%)** | - | 2 (6.9) | 1 (6.3) | 1 (20.0) |
| **rhinoplasty†, N (%)** | - | 3 (10.3) | 2 (12.5) | 0 (0.0) |
| **sinus surgery†, N (%)** | - | 6 (20.7) | 1 (6.3) | 0 (0.0) |
| ***OE MORPHOLOGY*** | | | | |
| **normal (%OE)** | 23.04 ± 4.69[a] | 14.47 ± 3.57[ab] | 10.79 ± 3.46[ab] | 1.64 ± 1.64[b] |
| **goblet (%OE)** | 33.44 ± 7.50 | 38.06 ± 5.65 | 41.79 ± 8.17 | 39.2 ± 15.40 |
| **squamous (%OE)** | 35.97 ± 7.36 | 36.25 ± 6.66 | 32.47 ± 9.04 | 20.0 ± 20.0 |
| **erosion (%OE)** | 8.08 ± 2.69 | 11.56 ± 4.51 | 14.94 ± 6.06 | 39.16 ± 16.57 |
| **OMP-ir OSNs†, N biopsies (%)** | 9 (45.0) | 7 (24.1) | 4 (25.0) | 1 (20.0) |
| **no OMP-ir†, N biopsies (%)** | 4 (20.0) | 8 (27.6) | 7 (43.8) | 2 (40.0 |
| ***INFLAMMATION*** | | | | |
| **eosinophils (#/mm OE)** | 0.38 ± 0.16[a] | 1.39 ± 0.56[a] | 1.50 ± 0.79[a] | 6.74 ± 3.74[b] |
| **macrophages (#/mm OE)** | 25.95 ± 6.32 | 16.50 ± 4.40 | 10.76 ± 3.12 | 8.67 ± 5.31 |
| **neutrophils (#/mm OE)** | 36.85 ± 12.90 | 22.38 ± 5.95 | 16.06 ± 6.10 | 15.6 ± 11.05 |

± standard error; non-overlapping letter superscripts reflect group differences at $p \leq 0.05$

† = differences were analyzed using Fisher's exact test; all other pairwise comparisons were by Fisher's LSD. ALLERGY = tested positive on at least one allergen sample

‡ = based on the University of Miami CRS staging system[32]; DIAGNOSED POLYPS = profound polyps with or without visible airway; EARLY POLYPS = observed in both ostiomeatal complex and sphenoethmoidal recess; ENDOSCORE = total score for endoscopic exam, range 0 – 14; ANTETH = degree of sinus mucoperiosteal thickening in both anterior ethmoid, range 0 – 8; POSTEH = degree of sinus mucoperiosteal thickening in both posterior ethmoid, range 0 – 8; CTSCORE = total score for both sides, range 0 – 27. In rows without letter superscripts, the main effect for group was not significant in the overall ANOVA or Fisher's exact test.

ANOVA = analysis of variance; BM = basement membrane; CRS = chronic rhinosinusitis; OMP-ir = olfactory marker protein immunoreactivity; OSNs = olfactory sensory neurons; OE = olfactory epithelium; PEA = phenylethyl alcohol.